REPORT DOCUMENTATION PAGE

AFRL-SR-BL-TR-01-

0415

1. AGENCY USE ONLY (*Leave Blank*)	2. REPORT DATE	3. REPORT TYPE AND DATES COVERED
	April 20. 2001	Final Technical Report - 01/15/97 - 12/31/2000

4. TITLE AND SUBTITLE
Mechanisms and Mechanics of Interface Fracture in Metal Matrix Composites Controlling Overall Performance

5. FUNDING NUMBERS
G F49620-97-1-0347

6. AUTHORS
A. S. Argon, Quentin Berg Professor of Mechanical Engineering, Room 1-306, MIT

7. PERFORMING ORGANIZATION NAME(S) AND ADDRESS(ES)
Massachusetts Institute of Technology, Mechanical Engineering Department

77 Massachusetts Avenue
Cambridge, MA 02139

8. PERFORMING ORGANIZATION REPORT NUMBER
1

9. SPONSORING / MONITORING AGENCY NAME(S) AND ADDRESS(ES)
AFOSR/NA (Dr. Thomas Hahn)
Directorate of Aerospace and Materials Science
801 N. Randolph St.
Arlington, VA 22203

10. SPONSORING / MONITORING AGENCY REPORT NUMBER

11. SUPPLEMENTARY NOTES

12a. DISTRIBUTION / AVAILABILITY STATEMENT
UNLIMITED

12b. DISTRIBUTION CODE

13. ABSTRACT *(Maximum 200 words)*

In certain metal matrix composites, and specifically in Al alloy aligned fiber Al_2O_3 composites the debonding response of interfaces adjacent to fiber fractures, in mixed tension and shear has important influences in the strength and toughness of the composite. Coarsening of interface precipitates offers close control of the level of debonding on such interfaces. In the present research computational models were developed for the interface debonding response under mixed tension/shear: traction/separation response of the interfaces. Additional experiments were also performed on a prototype composite of Al with Al_2O_3 fiber preforms which demonstrated quite considerable toughening effects by fiber bridging in the arranged samples.

20010731 026

14. SUBJECT TERMS
Metal Matrix Composite; interface debonding ; computer simulation of debonding; Al 2 0 3 composite with fiber pre-form

15. NUMBER OF PAGES
3

16. PRICE CODE

17. SECURITY CLASSIFICATION OF REPORT	18. SECURITY CLASSIFICATION OF THIS PAGE	19. SECURITY CLASSIFICATION OF ABSTRACT	20. LIMITATION OF ABSTRACT
UNCLASSIFIED	UNCLASSIFIED	UNCLASSIFIED	UNLIMITED

ROLE OF CONTROLLED DEBONDING ALONG FIBER/MATRIX INTERFACES IN THE STRENGTH AND TOUGHNESS OF BOTH ALIGNED AND UNALIGNED-FIBER/METAL-MATRIX COMPOSITES.

(AFOSR Grant F49620-97-1-0347)

A. S. Argon
Mechanical Engineering Department
Massachusetts Institute of Technology
Cambridge, MA 02139

1. Introduction

While metal-matrix composites offer remarkable potential for applications in load bearing structural elements at intermediate to high homologous temperatures, short of long term creep conditions in the metal matrix, barring a few outstanding examples such as diesel engine piston heads, this potential has rarely been fully realized. This is because the development of these composites has largely been fragmented into pre-conceived areas of importance such as fiber development, matrix/fiber compatibility, processing and a limited set of performance controlling factors, and the like, rather than being based on coherent considerations of the major factors and their interactions that govern composite performance. Particularly in the area of achieving combined high axial and transverse strength and high levels of work of fracture, very substantial improvements are possible through a newly developed process of interface structure control and its analysis. This process is based on placement of a pedigreed population of intermetallic compound precipitates on the fiber/matrix interface that provide a wide range of control of the interface traction/separation relationship, and thereby achieve desired levels of interface debonding that governs subsequent matrix ligament rupture and resistance to axial shearing off.

In this report the details of the main findings of both composite micromechanics models specially developed for this purpose, and supporting experiments, carried out under AFOSR support are described.

2. Basic Mechanisms and Modeling Concepts

In metal-matrix composites with strong aligned fibers, having only small variability in strength, final fracture is often by the planar fracture of parallel fibers as depicted in Figure 1 as a so-called Type A fracture, bridged by Type B-shear fractures. The fracture toughness, or in this case, the specific work of fracture, U_A, is governed by the plastic work of metal ligament rupture following the fracture of the fibers. This sequence of fracture process involving the fracture of fibers, followed by matrix ligament rupture that can be nurtured in metal matrix composites permits the attainment of an attractive combination of both strength and fracture toughness across the fibers. The fundamental first order order relation that governs the post-fiber-fracture-toughness, U_A, can be given as [1].

$$U_A = \frac{1}{\sqrt{3}}(1 - v_f)\sigma_0 L_D \tag{1}$$

where v_f is the fiber volume fraction, σ_0 the tensile plastic resistance of the metal matrix and L_D the, all important, debonding length of the fiber from the matrix around the principal fiber breaks. A tenacious adhesion of fiber to matrix results in a

very short L_D giving a very low U_A while a very low level of fiber to matrix adhesion gives a debond length L_D at a level that can exceed the natural necking length of the metal ligaments. While such low adhesion results in the largest level of U_A it also seriously reduces the transverse tensile strength of the composite. An optimum condition of adhesion can be reached by tailoring the adhesive strength to give a close approach of L_D to the natural necking length. This is achievable by a process of controlling the level of coarsening of interface precipitates on the fiber/matrix interface. In the specific metal-matrix system incorporating polycrystalline $Al_2 0_3$ fibers and an aluminum alloy matrix with Al_2Cu precipitates the latter adhere well to the matrix but not to the fiber. The coarsening of interface precipitates results in the increase of the scale of inter-precipitate metal ligament spacings which govern the ductile dimple fracture work along the interface, upon precipitate debonding all depicted in the various parts of Fig. 1. The figure also shows a micrograph of the fractured composite, with broken fibers and ruptured metal ligaments. In the AFOSR-supported research program both the experimental phase of the fracture scenario described above as well the development of a composite micromechanics model was pursued. In the composite micromechanics model important collaboration was obtained from C. F. Shih of Brown University (at that time) and X. H. Liu. The experimental research was pursued by M. L. Seleznev and later by J. Gregory.

In Part 3 of this report a brief outline of the composite micromechanical models is given,the full form of which has been published earlier [1]. In Part 4 of the report an experimental study is described in which the basic tension/shear fraction/separation response for the debonding of the fiber/matrix interfaces is determined in scaled-up prototype form.

In Part 5 of the report a separate experimental study is described in which the behavior of aluminum matrix composites with unoriented fiber preforms has been considered in some detail to assess to possibility of obtaining similar beneficial results in unoriented-fiber composites. Part 4 and 5 constitutes the SM Thesis of J. Gregory [2].

Part 6 furnishes a brief discussion evaluating the potential of the findings. Statistical information related to co-workers, to the publications arising from the research, to degrees granted, and to the various lecture presentations are listed in Section 7.

3. Composite Micromechanics Models

3.1 The tension /shear: traction/seperation model

Figure 2 shows the basic plane-strain idealization of the boundary value problem for the tension/shear: traction/separation model of fracture along a fiber/matrix interface in which the fracture process initiates with debonding of the precipitates from the fibers along the planar interfaces, *e-g*, (actually considered in the model to be along the semi-cylindrical interface *e-f-g* for computational ease). The elastic response of both the matrix (upper-half space) as well as the fiber (lower half space) is considered faithfully. The plasticity of the matrix is approximated by a power-law form, tailored properly to the visco-plastic response of the precipitation-strengthened aluminum alloy matrix. An appropriate tensile debonding strength between precipitates and fibers of 1.0 GPa was considered in the model.

Figure 3 shows a typical computational output of the tension/shear: traction/separation behavior of the interface in which the angle between the imposed shear direction and tension was $\varphi = 30^0$. Frame (a) shows the actual tension/separation and the shear-

traction/shear-displacement profile while (b) shows several states of the rupture process in the inter-precipitate ligaments where the numbers relate to the points on the separation profile of frame (a).

Additional profiles considered were for $\varphi = 0^0$, 60^0, and 85^0.

3.2 Composite fracture under axial separation conditions parallel to the fibers.

Figure 4 shows the basic boundary-value- problem (BVP), again in plane-strain idealization for the evolution of inter-fiber rupture resistance upon fiber fracture. In this model which pertains to a realistic condition of $v_f = 0.5$, the fiber/matrix debonding in response to the evolving mix of tensile and shear separation conditions is considered. As the matrix ligament (left column in Fig. 4) ruptures a more generic tension/shear: traction/separation dependence has been employed for the debonding of the fiber-matrix interface. The elasticity of both the matrix and the fiber have been considered properly to relate to Al and Al_20_3 respectively and the visco-plastic response of the Al matrix has again been approximated by a power-law form. The overall response has been considered on a relatively wide range of parameters which is too broad to be present here. The overall finding is summarized in Fig. 5 which gives the dependence of the work of fracture, U^*, of the composite across the fiber direction (normalized with the product of the plastic resistance of the matrix, σ_0, the strain at yield, ϵ_0, and the square of the matrix ligament half thickness, b), on the effective interface debond work Γ_0, (normalized with the product of $\sigma_0 b$). The figure shows that the best results are obtained for $\Gamma_0/\sigma_0 b = 0.25$. Comparison of findings with experiments indicate that this condition is readily realizable through matrix aging. [1]

The earlier experiments that have been the principal stimulus to the AFOSR-supported research program have been described elsewhere [3] but are also reviewed briefly in [1].

4. Experimental Determination of the Tension/Stress: Traction/Seperation Response

While many authors have invoked the use of a traction: seperation (TS) law in either tension or in sheer, or in a combination [4, 5] to explain seperation at an interface, and computational models have been developed, including the one presented briefly in Section 3.1 above, there are no direct experimental measurements for such behavior, particularly for the ductile cavity growth mode that is depicted in Fig. 1. The principal difficulty in the measurement of a realistic TS behavior is the difficulty of stably following the declining portion of the behavior shown in Fig. 3. To experimentally follow such a declining traction behavior resulting from the debonding of an interface in a reasonable size laboratory specimen where the debonding distance is of the orderof $10^{-6}m$ would require a testing system with a stiffness that would be several orders of magnitude in excess of what is usually available. Since the TS law to be measured results from continuum plastic ligament rupture the experimental strategy was to coarsen the "precipitate" spacing, D, in Fig. 3 from the *micron* range to the *mm* range, while maintaining constant the area fraction of "precipitates" on the interface. This can be readily accomplished in a scaled-up prototype experiment where the separating interface precipitates of Al_2Cu of roughly 1.0 micron spacing in the actual system were replaced with a regular pattern of readily debonding circular dots of *mm* spacing imprinted on a planar model interface of Al_20_3 (sapphire) and super pure Al. This would accomplish achieving the same peak tractions of

the real system but with the separation displacement increased by three orders of magnitude, permitting the experimental measurement of the TS law with a standard tension/torsion specimen arrangement shown in Fig. 6, in which the sapphire single crystal disk imprinted with a dot pattern of circular Fe spots of mm size and spacing was diffusion bonded to a super pure aluminum section to form a scaled up version of the actual interface between the matrix and fiber in the real system. In the prototype the circular Fe dots act as poorly bonded sites to undergo ready separation to produce the 2-D plastic dimple rupture process under various combinations of tension and shear. In this manner several moderately successful experiments were carried out in the tension/separation mode. Figures 7a and 7b show such an example of a measured TS law and a micrograph of the scaled up plastic dimple fracture. [2]. While the required experimental procedure for obtaining the diffusion bonded scaled-up interfaces across a thin-walled tension/torsion specimen was achieved, the available time within a Masters degree program of Gregory was insufficient to carry out a full complement of tension/shear: traction/separation responses to compare with the modeling study presented in Section 3.1 above.

5. Experiments with Al/Al_20_3 Composites Containing Infiltrated Fiber Preforms

5.1 Overview and Material System

To explore the applicability of the special toughening mechanism based on the control of the debonding condition of fibers from the matrix along precipitate-bearing interfaces outlined in Section 2, a set of Al/Al_20_3 composites were prepared in which the Al_20_3 fibers were arranged randomly in fiber pre-forms which were infiltrated with an Al, $5\%Cu$ alloy through casting. The fiber pre-forms that were used to manufacture the metal-matrix composites of , Fibralloy Al 20, were produced by Thermal Ceramics and were composed of Saffil RF grade alumina fibers, held together with small amounts of binder agents. The median fiber diameter was 3.0 μm and the approximate median fiber length was 50-70 μm. The composite was cast using pressure infiltration of the Al-$5\%Cu$ alloy at Metal Matrix Cast Composites, Inc. The manufacturing process resulted in blocks of material containing 0.2 volume fraction of fibers that could then be cut to obtain test specimens.

Once the individual test specimens were cut from the MMC blocks, the samples were subjected to various heat treatments meant to change the size and distribution of the precipitates on the fiber/matrix interface by coarsening. The specific heat treatment applied to each specimen followed general procedures of precipitate coarsening, but in general most of the specimens underwent a standard T7 heat treatment while some other specimens underwent a T6 heat treatment. Any overaging was conducted at 350^o C after the initial heat treatment to obtain well dispersed interface precipitates.

5.2 Probing for mechanical response

The response of the cast composite samples were probed primarily in uniaxial tension to determine changes in deformation resistance and by forms of fracture mechanics approaches to determine fracture resistance.

Figure 8a shows stress-strain curves of the unreinforced cast aluminum alloy matrix component for a range of aging histories from the base heat treatments of T6 and T7, followed by overaging schedules up to 288 hours at 350C. Figure 8b shows the corresponding results for the Al_20_3 fiber pre-form filled composite samples having a fiber volume fraction of 0.2. Comparison of the two figures indicates that for the

fiber pre-form-modified matrices the yield strengths of the T6 and T7-treated material were about 17% higher than those of the unmodified cast alloy. There was also a slight increase in the Young's modulus of the fiber-modified composites, roughly commensurate with what could be expected from a lower bound estimate. While these marginal improvements in the uniaxial tensile resistances were interesting they would hardly constitute a strong stimulus for fiber incorporation in this random pre-form manner.

A more interesting and important aspect of random fiber modification was noted in the fracture behavior. This effect is shown in Fig. 9 which gives the load/crack-openingdisplacement (L/COD) curves for a peak aged T7 composite alloy and for too additional cases with 10 and 100 hours of over-aging treatments at 350C. Clearly, the T7 composite has very little fracture resistance, showing unstable fracture response well characterizable by a critical K_I, while the over-aged alloys show a very dramatic long range fiber pull-out behavior indicating no instability in the compact specimen geometry and little notch sensitivity - all compatible with a fracture response with substantial critical crack opening dispercement (CCOD). Therefore, to provide a meaningful comparison the fracture resistance of all three cases have been evaluated uniformly by a standard J integral approach based on [6].

$$J = \alpha\epsilon_0\sigma_0(1-\varphi)ch_1(\frac{a}{b}, n)(\frac{P}{P_0})^n \tag{2}$$

where the relevant parameters have well know usual interpretations given in standard texts [6, 7] related to compact specimen geometry, and non-linear (elasic-plastic) material behavior based primarily on the Al metal matrix, with φ being the precipitate volume fraction. The relevant values related to these 3 tests are given in Table I. Examination of the last line in the table shows the dramatic improvement of toughness in the over-aged composite, over the composite given only the standard T7 base treatment. While the differences in the J levels for the T7/10 and T7/100 composites are probably not too reliable in view of the very similar L/COD curves given in Fig. 9, their improvement over the T7 treated material is striking and well featured in Fig. 9. The differences between these two extreme cases is also reflected in the SEM micrographs of Fig. 10a and 10b, giving the fracture surface features for the T7/10 and the T7/100 composites respectively. In Fig. 10a the ductile dimples on the interfaces of the fibers are very small showing in addition regions of poor adhesion of the matrix on the fibers. The dimples in Fig. 10b, are in comparison much larger and show a state of well adhered matrix on the fibers. While these micrographic evidences of difference are striking, the very beneficial post-peak tail in opening displacement shown in Fig. 9 for the overaged samples indicates that the lower peak loads of the overaged samples have permitted also considerable rotation of separated fiber segments and associated fiber bridging across the opening crack faces.

6. Discussion of Findings

The principal findings based on the computational models discussed in Section 3 and the experimental results summarized both in earlier publications [1, 3], as well as those presented in Sections 4 and 5, indicate that in certain instances with metal matrix composites manipulation of the interface structure between fibers and matrix through aging of interface precipitates can give a very useful means of tailoring debonding response along interfaces. This interface debonding response as explored in detail through micromechanical computational models [1] can achieve very attractive combinations of axial strength and fracture resistance of cracking across the fibers together with very good levels of transverse strength. The micromechanical

composites models prescribe ranges of precipitate coarsening and influences of other elastic-plastic matrix response characteristics for achieving optimum results.

In a related experimental effort procedures were developed for the experimental determination of fundamental tension/shear: traction/separation responses across interfaces that closely resemble the forms of response incorporated into the micromechanical computer models.

In yet a further experimental excursion, the potential utility of manipulation of interface response in metal-matrix composites with random fiber pre-forms was also explored. These experiments indicated that while the gains in overall tensile response related to elastic propeties and plastic flow resistance are marginal and not worth the effort, the gains in fracture resistance were very substantial due to the development of substantial post-peak-load crack opening displacements in crack growth that must be related to R-curve behavior.

TABLE I

Quantities used in *J* integral evaluation of infiltrated fiber preform fracture experiments

HT/0 (hrs.)	T7/0	T7/10	T7/100
a (mm)	22.1	22.0	22.0
b (mm)	39.6	39.5	39.7
ϕ	0.03	0.03	0.03
h_1	0.629	1.161	1.178
P (kN/m)	217.2	196.1	192.0
P_0 (kN/m)	838.6	156.3	118.1
η	0.139	0.140	0.140
ε_0 (%)	0.35	0.064	0.051
σ_0 (MPa)	245.34	45.37	33.68
α	1.14	1.63	1.56
n	8.40	3.53	3.42
J (J/m^2)	0.032	2601.75	4574.54

$\varepsilon=\alpha\varepsilon_0(\sigma/\sigma_0)^n$

References

1. A. S. Argon, M. L. Seleznev, C. F. Shih and X. H. Liu, *Internatl. J. Fracture*, **93**, 351 (1998).

2. J. R. Gregory "The role of precipitates on fiber/matrix interfaces in metal-matrix composites", S.M. Thesis in Mechanical Engineering, M.I.T. Cambridge, MA (2000).

3. M. L. Seleznev, J. A. Cornie and F. A. Armantis, Jr. *J. Mater. Engng. Performance*, **2**, 347 (1993).

4. A. Needleman, *J. Appl. Mech.*, **54**, 523 (1987).

5. J. R. Rice, G. E. Beltz, and Y. Sun, in "Topics in fracture and fatigue", edited by A. S. Argon, Springer, New York, p. 1, (1992).

6. V. Kumar, M. D. German and C. F. Shih, "An engineering approach for elastic-plastic fracture analysis" Technical Report NP-1931 General Electric Co. Corporate R&D (1981).

7. T. L. Anderson, "Fracture mechanics: fundamentals and applications" (second edition) CRC Press, Boca Raton, Florida (1995).

7. Statistical Information

7.1 Personnel:

A. S. Argon, principal investigator, Quentin Berg Professor of Mechanical Engineering, M.I.T.

J. R. Gregory, graduate research assistant, Mechanical Engineering Department, candidate for Masters Degree.

X. H. Liu, graduate research assistant, Division of Engineering, Brown University, doctoral candidate, supervised by C. F. Shih

M. L. Seleznev, post doctoral associate, Mechanical Engineering Department, M.I.T.

C. F. Shih, Professor of Mechanical Engineering, Division of Engineering (at the time (presently at the Singapore National University).

7.2 Industrial Collaborations:

The research effort enjoyed extensive collaboration from Metal-Matrix Cast Composites Inc. (MMCC) of Waltham, MA in material preparation through the active support of Dr. James A. Cornie, company president.

7.3 Technical presentations

- A. S. Argon, "Interfacial Engineering in Metal-Ceramic Composites" at the Gordon Conference on Complex Ceramic Microstructures: Properties by Design", Aug. 4-9 (1996, at Kimball Union Academy, Meriden, NH.
- A. S. Argon, "Toughening of Metal Matrix Composites Through Control of Interface Toughness Between Fibers and Matrix", invited lecture at the TMS Symposium on 'Ductile Fracture", Feb. 10, 1997, at Orlando, Florida.
- A. S. Argon, M. L. Seleznev, C. F. Shih and X. H. Liu, "Mechanism and Mechanics of Debond Fractures along Metal-Matrix Composite Interfaces", Keynote lecture at the 9th International Conference on Fracture, April 1-5, 1997, at Sydney, Australia.
- A. S. Argon, M. L. Seleznev, C. F. Shih and X. H. Liu, "Toughness Control of Al/Al_20_3 Fiber Composites Through Interface Particle Coarsening: Experiments and Modeling", Keynote address, at the ASM Symposium on "Mechanisms and Mechanics of Composite Fracture: Fiber Reinforced Composites", Oct. 12, 1998, at Chicago, IL.
- A. S. Argon, "Optimization of Strength and Toughness of Al/Al_20_3 Fiber Composites: Experiments and Modeling", Keynote address at the Special Symposium on "Inegration of Material Process and Product Design", (a conference in honor of Owen Richmond) Oct. 19, 1998, at Seven Springs PA.
- A. S. Argon, "Comprehensive View of Toughness Mechanisms"; Keynote Lecture at the"Seventh Annual International Conference on Composites Engineering (ICEE7), "July 3, 2000 at Denver CO.

7.4 Publications

1. A. S Argon, M. L. Seleznev, C. F. Shih and X. H. Liu 'Mechanisms and mechanics of debond fractures along metal-matrix composite interfaces", in *Advances in Fracture Research*, edited by B. L. Karihaloo, Y.-W Mai, M. I. Ripley and R. O. Ritchie, Pergamon Press: Oxford vol. 5, pp. 2377-2389 (1997).
2. A. S. Argon, M. L. Seleznev, C. F. Shih and X.H. Liu, "Role of controlled bonding along fiber/matrix interfaces in the strength and toughness of metal-matrix composites" *Internatl J. Fracture*, **93**, 351-371 (1998).
3. A. S. Argon, "Fracture: strength and toughness mechanisms", in *Comprehensive Composite Materials*, edited by A. Kelly and C. Zweben, volume 1 (edited by T.-W Chou) Pergamon Press, Oxford pp. 763-802, (2000).
4. J. R. Gregory, "The role of precipitates on fiber /matrix interfaces in metal matrix composites", S. M. Thesis in Mechanical Engineering, M.I.T. Cambridge, MA (2000).
5. J. R. Gregory and A. S. Argon "The role of precipitates on fiber/matrix interfaces in infiltrated $Al_2 0_3$ fiber pre-form-bearing metal-matrix composites" *J. Materials Science*, submitted for publication.

7.5 Honors and Awards received during the duration of present grant.

IMM/TMS Lecturer, 1998
ASME Nadai Medal, 1998
Staudinger-Duerrer Medal of the ETH-Switzerland, 1999
Southwest Mechanics Lecturer, 2000.

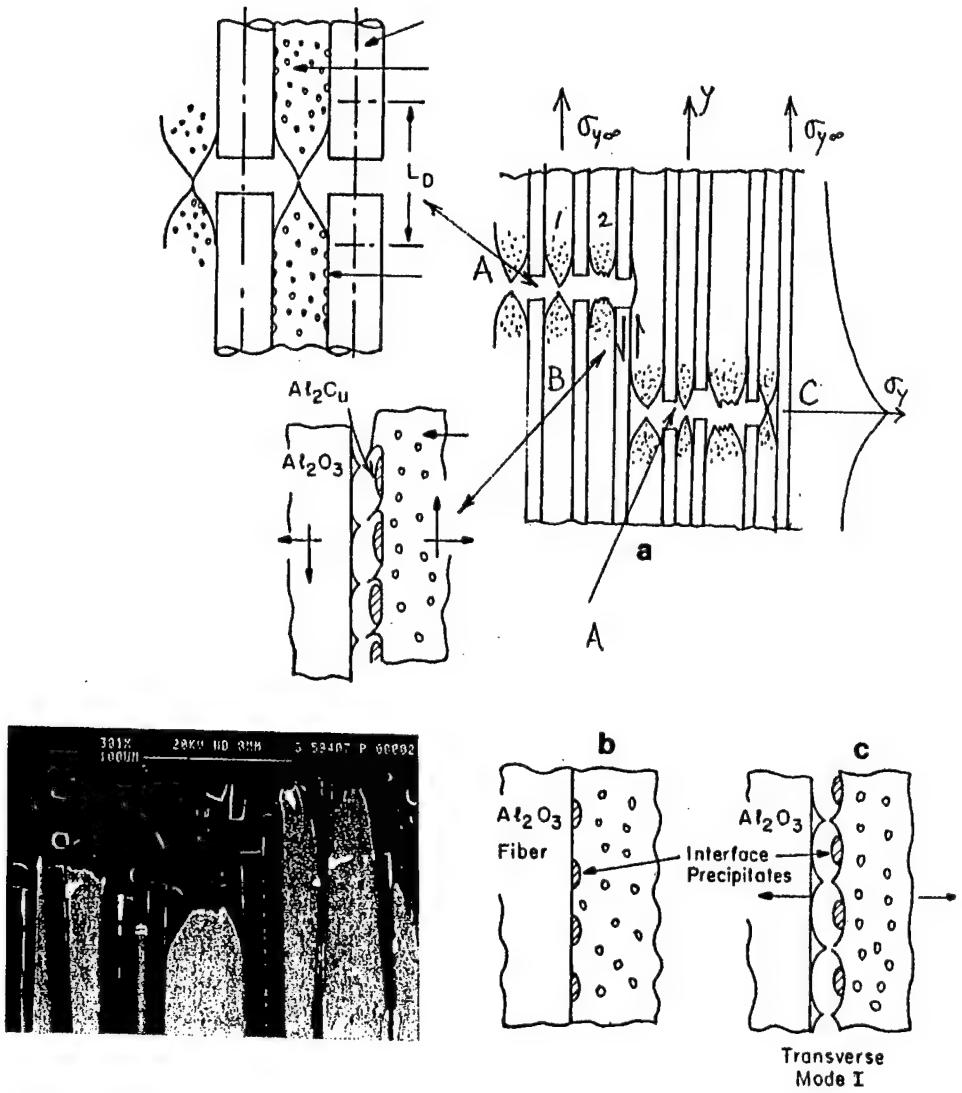

Figure 1. Forms of interface fracture in a metal matrix composite: (a) modes A of tensile, and B of simple shear fracture in a composite, with insets depicting the mixed mode of interface debonding fractures ocurring in modes A and B; (b) depiction of interface fracture of the composite, in the transverse direction.

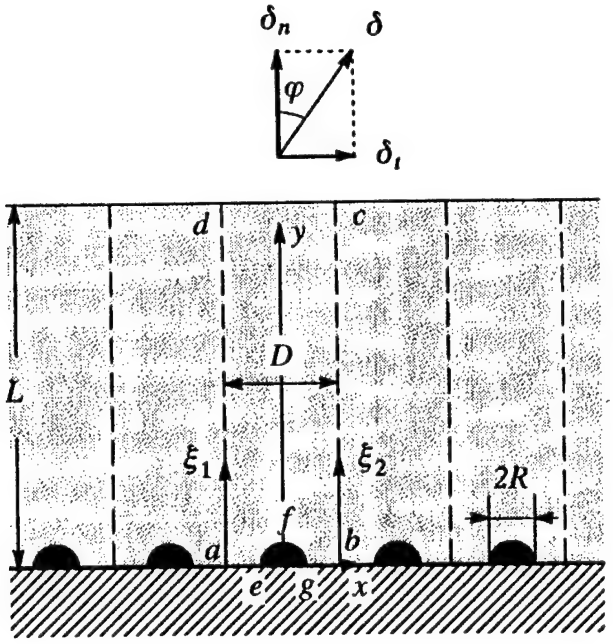

Fig. 2. The boundary value problem view of interface with a row of uniformly spaced semi-circular idealized precipitates.

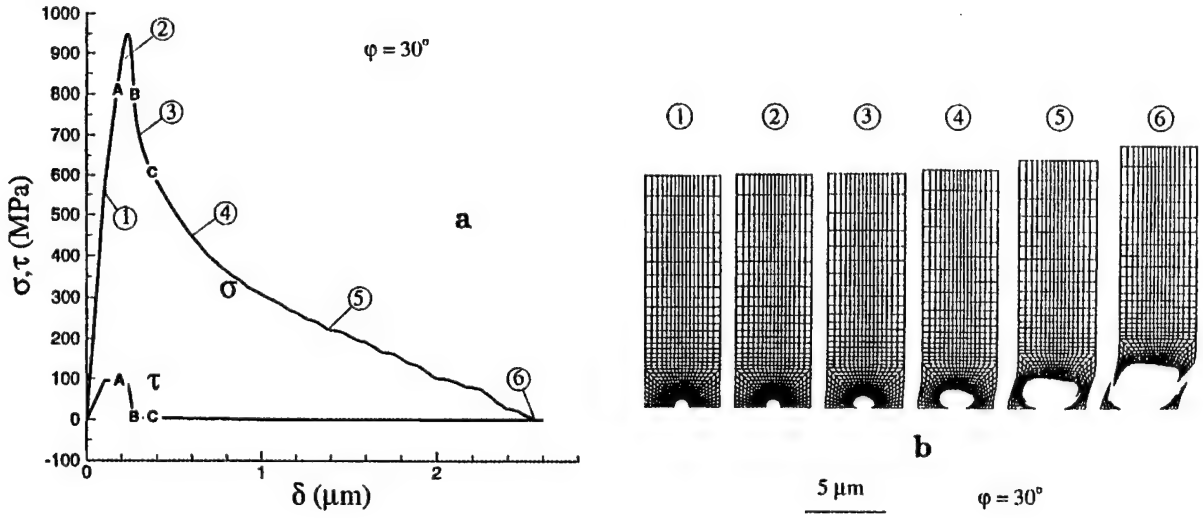

Fig. 3. (a) Calculated normal stress and shear stress versus axial loading displacement under combined tension and shear with phase angle $\varphi = 30^0$; (b) sequence of deformed configurations in mixed tension and shear loading. (from Argon, et al. 1998, courtesy of Kluwer, Academic Press)

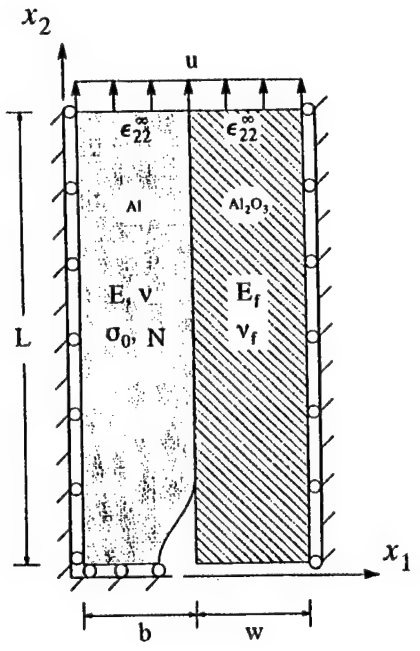

Fig. 4. BVP view of computational cell for longitudinal tension in a plane-strain idealization of composite fracture. The fiber is assumed to have fractured while the matrix is beginning to undergo rupture and in the process is pulling away from the fiber in a mixed mode of debonding.

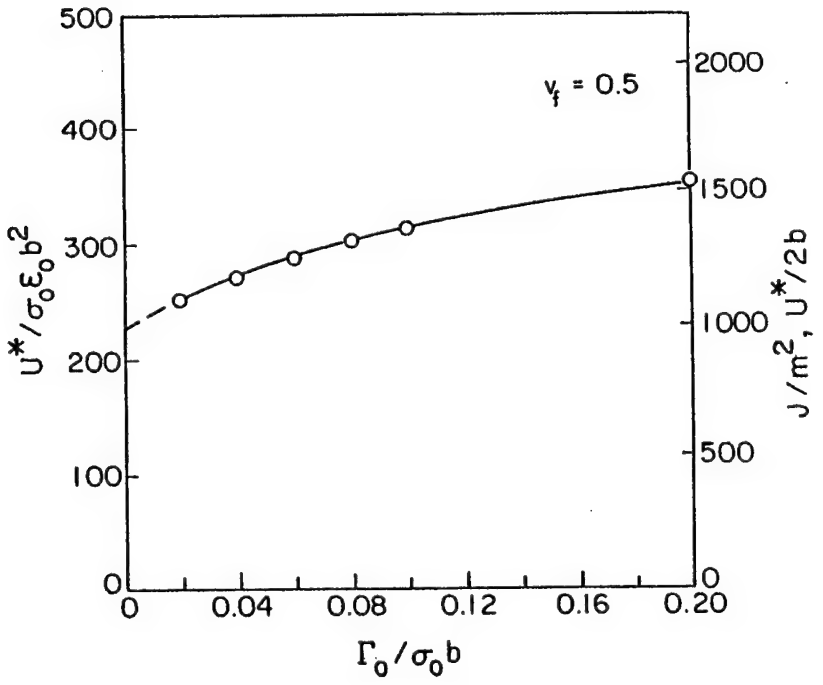

Fig. 5. Dependence of axial fracture energy U^* on the interfare debond energy Γ_0 at the fiber matrix interface, at a stage of local matrix ligament strain of $\epsilon = 1.5$ which is taken as a termination condition of ligament rupture. (from Argon, et al. 1998, courtesy of Kluwer, Academic Press)

Test Specimen Configuration and Exploded Assembly of Diffusion Bonding Set-up

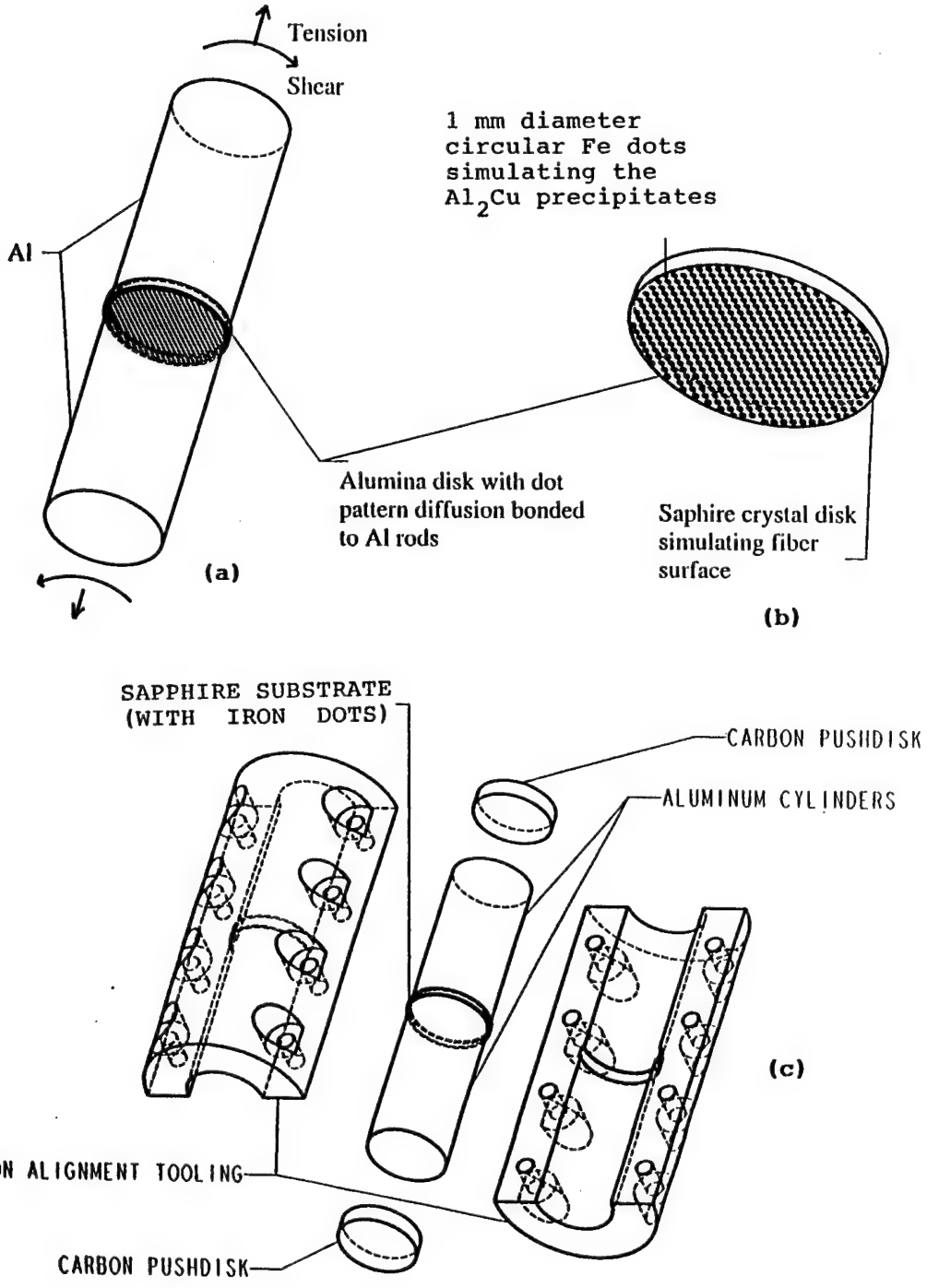

Fig. 6. Various views of the scaled-up prototype specimen to study the tension/shear/: traction/separation law experimentally in the laboratory: (a) the cylindrical tensions/torsion specimens with the sapphire disk, bearing the *Fe* dot pattern, diffusion bonded to two aluminum alloy ends to be loaded in tension and or torsion, (b) enlarged view of the sapphire disk with the circular pattern of *Fe* dots, (c) the exploded view of the graphite mold to hold parts together in diffusion bonding.

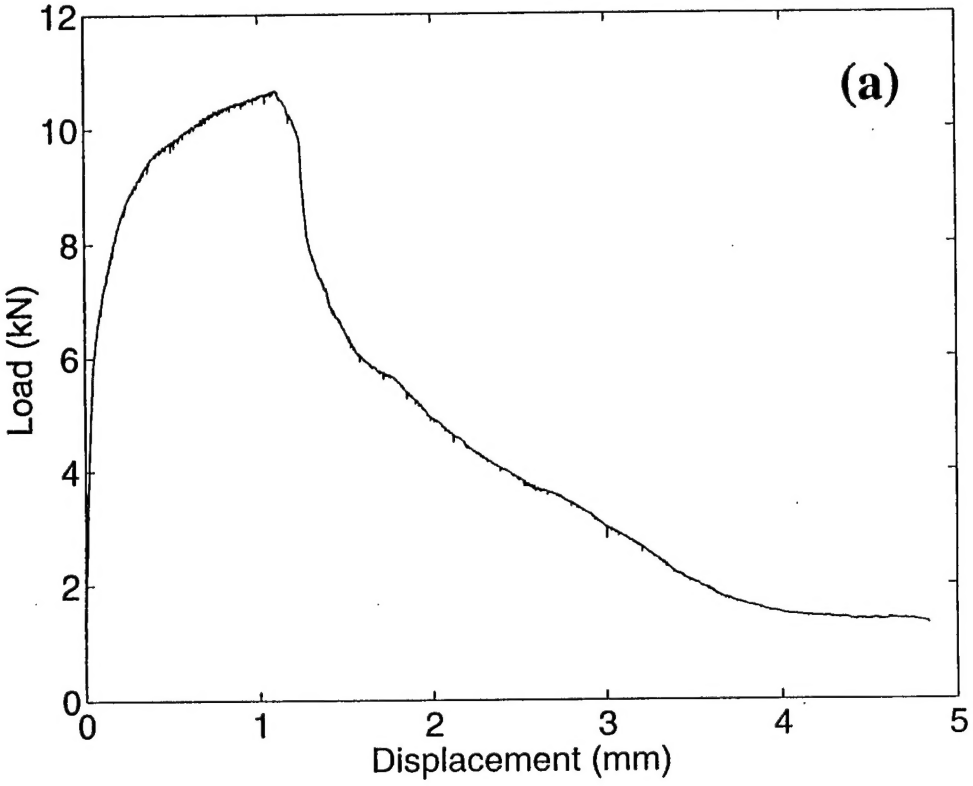

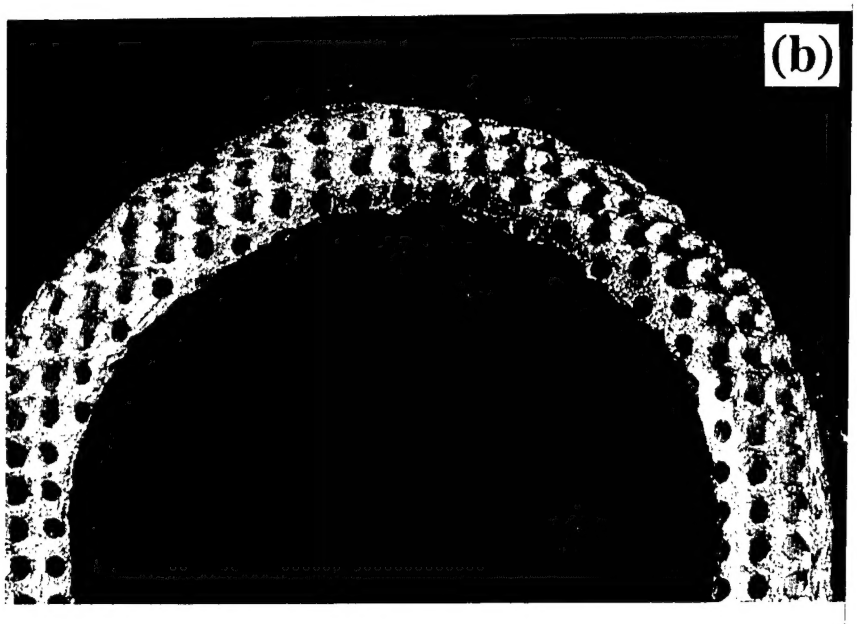

Fig. 7 (a) An experimentally determined traction (tension)/ separation displacement plot measured on a prototype scaled-up specimen of a thin walled tube, (b) the corresponding macro-graph showing separation at the Fe dots followed by ductile dimple rupture of the super-pure aluminum, diffusion bonded to the sapphire substrate; (the external diameter of the thin walled tube is 25 mm).

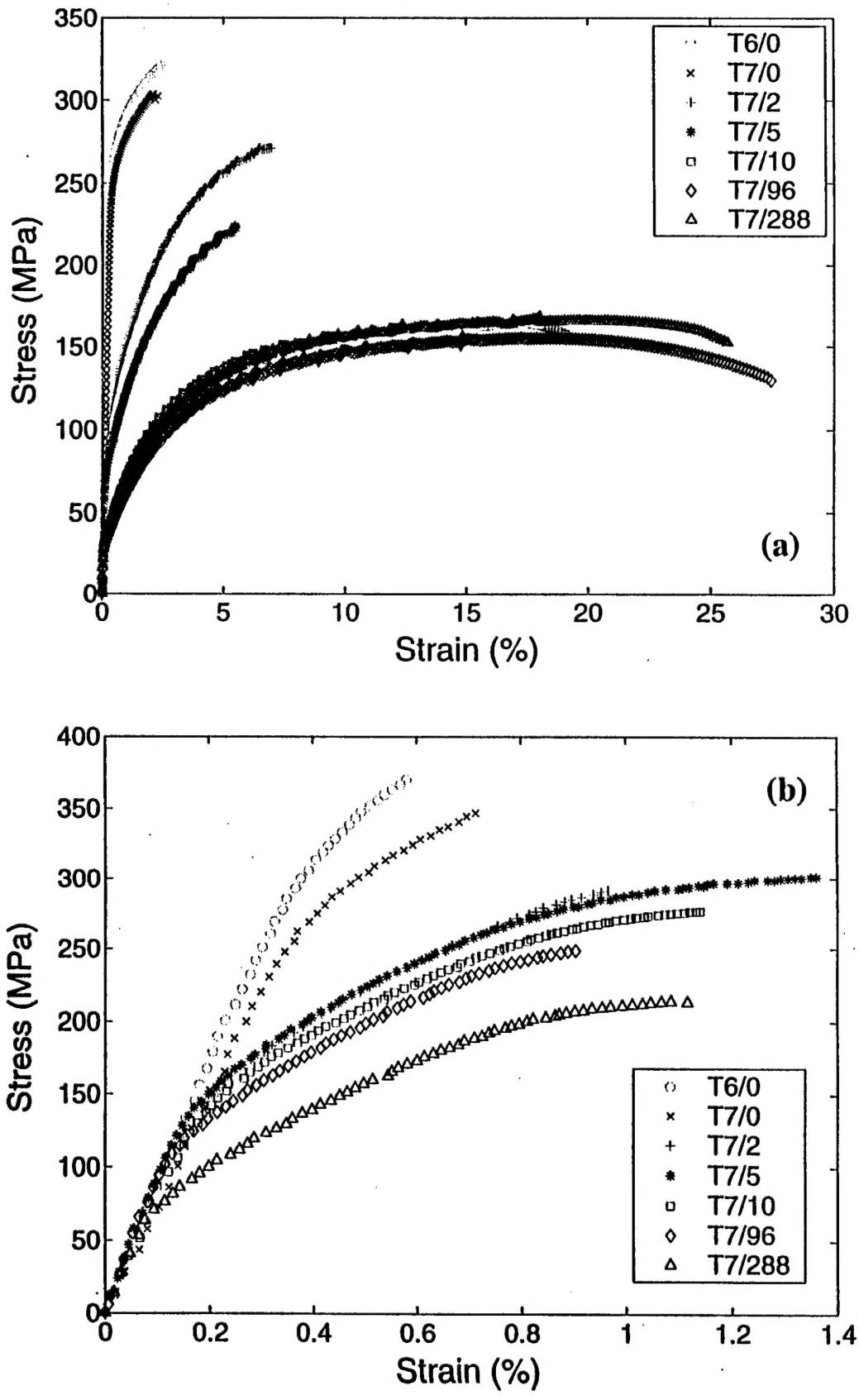

Fig. 8. (a) Stress-strain curves of unreinforced *Al* alloy matrix showing effect of various precipitation treatments and aging, (b) stress-strain curves of composite of *Al* alloy matrix with Al_2O_3 fiber pre-form at volume fraction of 0.2 of pre-form, with matrix being given various precipitation treatments as in (a).

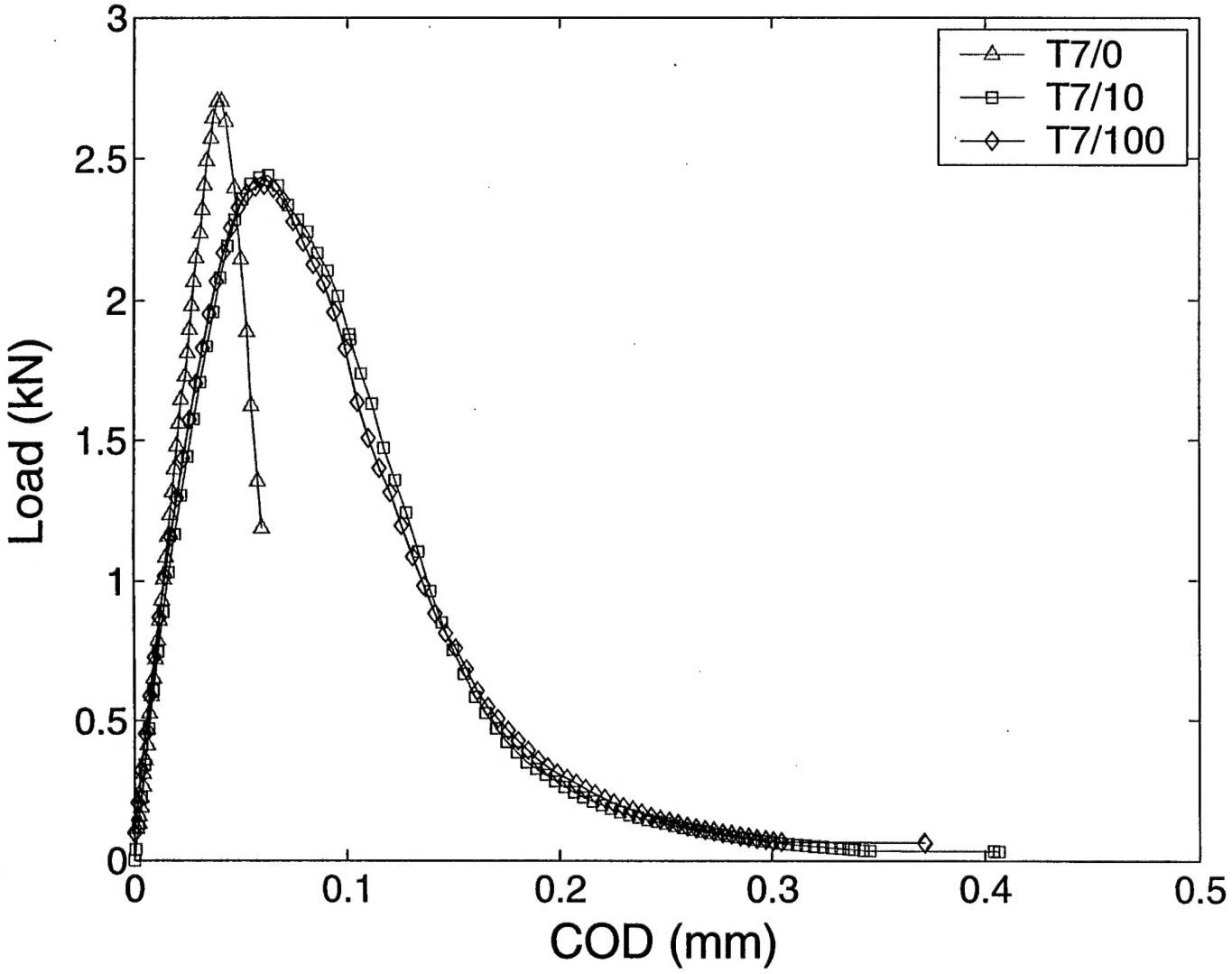

Fig. 9. Opening load/COD dependence in compact specimen type fracture mechnics response of cast composite with T7 heat treatment and no aging; and two samples with 10 hr. and 100 hr. overaging treatment at 350C, following the T7 treatment. The overaged samples show attractive R-curve type tough behavior with-substantial separation displacements .

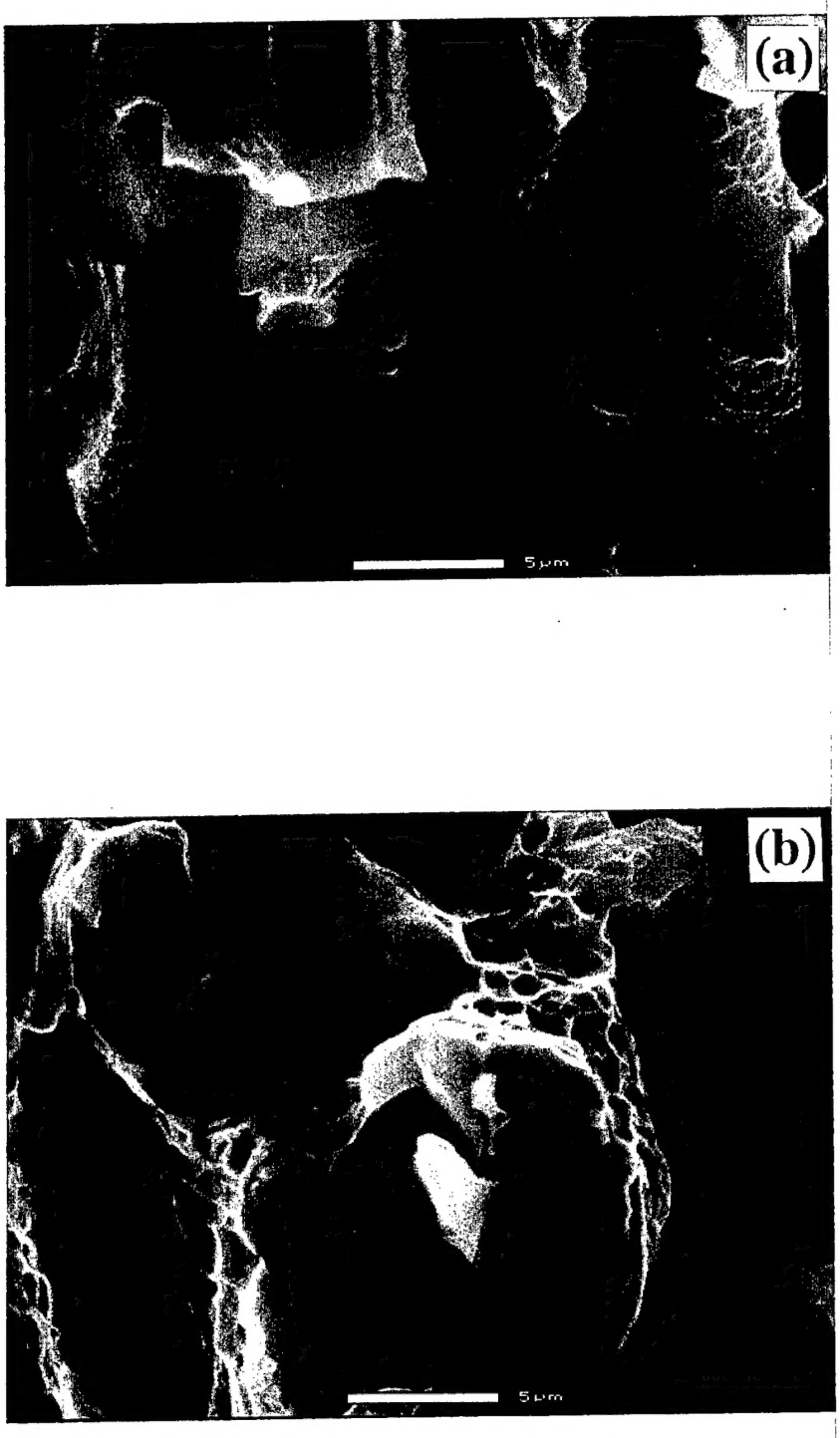

Fig. 10. SEM micrographs of fracture surfaces showing the different scales of dimple separation on fiber/matrix interfaces: (a) the T7 sample wihtout overaging, and (b) the T7 sample with 100 hr overaging at 350C.